

# *In Vivo* Measurements With Robust Silicon-Based Multielectrode Arrays With Extreme Shaft Lengths

Gergely Márton, Zoltán Fekete, Richárd Fiáth, Péter Baracsakay, István Ulbert, Gábor Juhász, Gábor Battistig, and Anita Pongrácz

**Abstract**—In this paper, manufacturing and *in vivo* testing of extreme-long Si-based neural microelectrode arrays are presented. Probes with different shaft lengths (15–70 mm) are formed by deep reactive ion etching and have been equipped with platinum electrodes of various configurations. *In vivo* measurements on rats indicate good mechanical stability, robust implantation, and targeting capability. High-quality signals have been recorded from different locations of the cerebrum of the rodents. The accompanied tissue damage is characterized by histology.

**Index Terms**—Neural microelectrode array, deep-brain electrode, silicon-based microelectromechanical system, spike sorting.

## I. INTRODUCTION

ELECTRODES, implanted into the central nervous system (CNS) are gaining increasing attention as they are being applied on a widening scale for medical purposes. With deep-brain stimulation, patients with Parkinson's disease or essential tremor can be treated [1], while cortical implants have been employed for control of prosthetic devices [2] and speech restoration [3].

In order to create electronic interfaces with the CNS, silicon-based microstructures are suitable candidates, since they can be provided with widely variable electrode configurations in a precise and reproducible manner, using highly biocompatible materials [4]. These devices allow good quality local field potential, single and multiple unit activity recordings [5], therefore they are frequently applied in experimental neurophysiology as well *in vivo*, in the CNS of small mammals,

Manuscript received December 12, 2012; revised April 9, 2013; accepted April 24, 2013. The work of A. Pongrácz was supported by the Bolyai János Grant of HAS. The work of I. Ulbert was supported by the French-Hungarian Grant TAMOP-4.2.1.B-11/2/KMR-2011-0002. This work was supported by the Hungarian Science Foundation under Grant OTKA K81354, and by the French-Hungarian Grants ANR-TÉT Neurogen and ANRTÉT Multisca. The associate editor coordinating the review of this paper and approving it for publication was Prof. Aime Lay-Ekuakille.

G. Márton, Z. Fekete, R. Fiáth, I. Ulbert, G. Battistig, and A. Pongrácz are with the Hungarian Academy of Sciences, Budapest 240050, Hungary (e-mail: marton.gergely@ttk.mta.hu; feket@mf.kfki.hu; fiath.richard@gmail.com; ulbert@cogpsyphy.hu; battisti@mfa.kfki.hu; pongracz.anita@ttk.mta.hu).

P. Baracsakay is with the Department of Biology, Eötvös Loránd University, Budapest H-1117, Hungary, and also with the Bay Zoltan Nonprofit Ltd. for Applied Research, Budapest H-1116, Hungary (e-mail: baracsakay@gmail.com).

G. Juhász is with the Department of Biology, Eötvös Loránd University, Budapest H-1117, Hungary (e-mail: gjuhasz@dec001.geobio.elte.hu).

Color versions of one or more of the figures in this paper are available online at <http://ieeexplore.ieee.org>.

Digital Object Identifier 10.1109/JSEN.2013.2260325

e.g. rodents. During experiments performed on mammals with larger brain, such as cats [6] or primates [7], silicon-based microelectrode arrays (MEAs) are typically implanted close to the brain surface, into the cerebral cortex. The application of such probes to access brain regions located more than 1 cm below the brain surface is highly unusual. For this purpose reinforced silicon-based probes of 1.05 cm have been presented [8]. In order to interface neural structures located deeper, wire electrodes are more frequently used, as their mechanical robustness is superior to silicon-based devices. However, they lack the benefits of multielectrodes manufactured with microelectromechanical system (MEMS) technology, such as precise, reproducible location of custom-designed electrodes with microscale dimension and good integration capabilities [9].

Polymer-based implantable neural electrode arrays, manufactured with MEMS technology, have also been reported [10], [11]. These flexible devices are able to provide smoother coupling with the neural tissue than silicon. They can adapt to the motions of the brain, thus they cause a less intense immune response and glial scar formation around the probe [12]. However, obtaining precise targeting during penetration into deep-brain regions is difficult or impossible without a more robust support structure [13] or a method that stiffens the implant at least during insertion [14], [15]. Acute experiments are not so sensitive for tissue response like chronic experiments, while easy, precise targeting is an important factor in both cases. These considerations brought the development of silicon-based, deep-brain multielectrode arrays for acute use into our attention.

In this work, we investigated whether the length of functionally appropriate silicon-based MEAs, manufactured using standard MEMS technology can be increased to a much greater scale. Extending shaft thickness and/or width can be a way for providing sufficient mechanical robustness for the implants, but increasing cross-sectional dimensions also increases invasiveness. In order to investigate the functionality of a probe with unusually large dimensions, we have performed *in vivo* experiments on rat cortex, hippocampus and thalamus. Although the access of these anatomical regions would not require such long shafts, we expect them to be very appropriate targets in order to find out whether these probes cause severe tissue damage, e.g. excessive loss of the nearby neurons. We have performed extracellular recordings in the targeted regions and employed a staining procedure, suitable for indication of damaged cells [16].

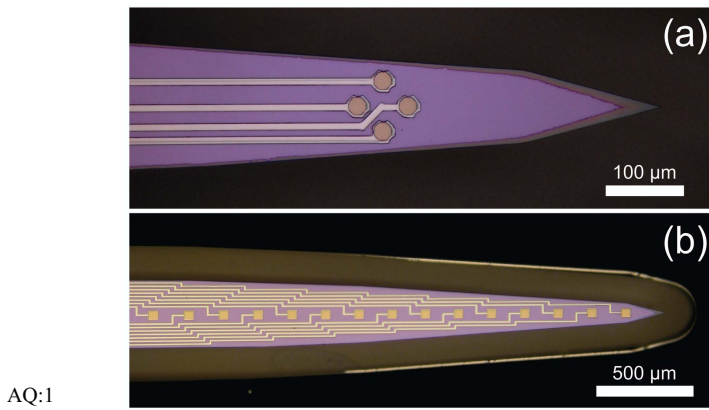


Fig. 1. (a) Tetrode and (b) linear electrode array configurations.

## II. MATERIALS AND METHODS

### A. Probe Design

Studies on the factors affecting mechanical properties of silicon-based neural implants have been published [17], [18]. We intended to manufacture stiff, rather than flexible, single-shaft probes, suitable for the penetration of the meninges (including the dura mater) and precise targeting. Shaft thicknesses were defined by the substrate silicon wafers (200  $\mu\text{m}$  and 380  $\mu\text{m}$ ), while their widths and lengths could be freely varied: 206  $\mu\text{m}$  and 400  $\mu\text{m}$  wide shafts with four different lengths (15 mm, 30 mm, 50 mm and 70 mm) were designed. These parameters have been thoroughly combined. Preliminary study of mechanical characterization of bare silicon probes (without electrodes) of such geometries has been previously presented by our group [19].

The recording electrodes (sites) on the probe tip were arranged as tetrodes (4 electrodes per probe in rhombus vertices) and linear arrays (12 or 16 sites in the midline of the front side of the shaft). Considering the latter, center-to-center distances of the 30  $\mu\text{m}$   $\times$  30  $\mu\text{m}$  and 50  $\mu\text{m}$   $\times$  50  $\mu\text{m}$  recording areas were 100  $\mu\text{m}$  and 200  $\mu\text{m}$ , respectively. Tetrodes were optimized for measuring single-unit activities, thus they were more compactly designed: the octagonal sites, 22  $\mu\text{m}$  in diagonal, were located 46  $\mu\text{m}$  distant from each other. We have formed electrode sites of platinum, which is a commonly used noble metal in this field, because of its biostability [20], [21].

### B. Microfabrication and Packaging

The fabrication technology of the deep brain multielectrodes is based on a single-side, three mask bulk micromachining process sequence that proceeded in three phases. The overall process flow is summarized in Fig 2. 200  $\mu\text{m}$  and 400  $\mu\text{m}$  thick, double-side polished (100) oriented 4-inch silicon wafers were used for the probe fabrication. The initial phase consisted of thin-film depositions to form the bottom insulating layers, the electrodes and output leads (Fig. 2.A). In the second phase the upper passivation layers were deposited and the contact holes, bonding pads and contour of the probe body were formed by different etching steps (Fig. 2.B). In the last phase deep reactive ion etching (DRIE) was used to define the

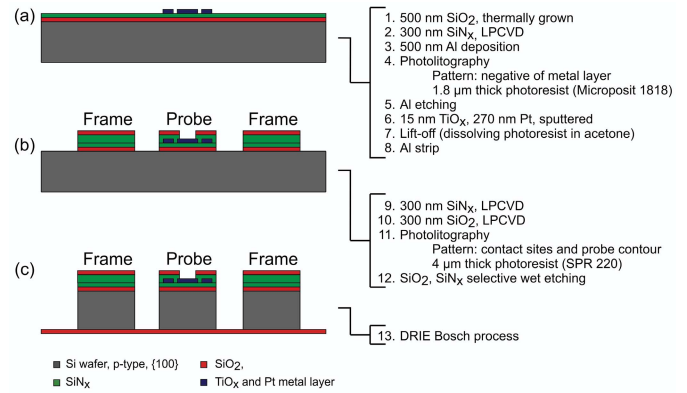


Fig. 2. Technological processes Forming lower insulator and patterned metal layers (a), upper insulator layers, opened at the sites (b), silicon dry etching with Bosch process (c).

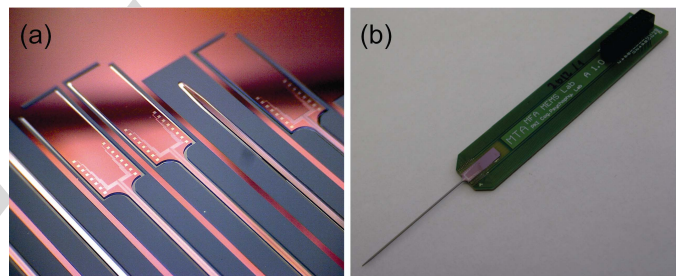


Fig. 3. (a) 16-channel multielectrodes on a micromachined silicon wafer. (b) A packaged silicon-based neural electrode on a PCB with shaft length of 3 cm.

probe shafts and bases (Fig.2.C) followed by the removal of the different masking layers and packaging of the probe.

Contact formation was obtained as follows. In the first step 500 nm thick SiO<sub>2</sub> layer was thermally grown on both sides of the wafer, followed by a deposition of 300 nm thick low-pressure chemical vacuum deposited (LPCVD) low stress silicon-nitride. The metal layer was then deposited and patterned by lift-off process. The lift-off structure composed of 1.8  $\mu\text{m}$  thick photoresist (Microposit 1818) layer over patterned Al thin film of 500 nm. The metal layer consisted of a 15 nm thick adhesion layer of TiO<sub>x</sub> and Pt. TiO<sub>x</sub> was formed by reactive sputtering of Ti in O<sub>2</sub> (Ar/O<sub>2</sub> ratio was 80:20) atmosphere. In the same vacuum cycle 270 nm thick Pt was sputtered on top of TiO<sub>x</sub>. The lift-off was accomplished by dissolving the photoresist pattern in acetone, this process was optimized by using water-cooled substrate holder which diminished the resist distortion during TiO<sub>x</sub>/Pt sputtering. Subsequently, the removal of Al patterns in four component etching solution and low pressure chemical vapor deposition of 300+300 nm thick SiN<sub>x</sub>/SiO<sub>2</sub> insulating layer stack occurred. Contact holes through the insulating layers were created by selective wet etching processes. By these processing steps, Pt lines insulated by SiN<sub>x</sub>/SiO<sub>2</sub> layers and formation of Pt contacts have been carried out.

For probe shaping a 500 nm thick Al layer was deposited on the front side and patterned by photolithography using 4  $\mu\text{m}$  thick SPR220 photoresist. The body of the probe was defined by Al wet etching. SPR220 photoresist was spun also

TABLE I

THE MAIN PROPERTIES OF THE MEAs, WHICH HAVE BEEN FUNCTIONALLY TESTED *in vivo*. MEASUREMENTS PERFORMED WITH PROBE NO. 2 AND 6 ARE PRESENTED IN DETAILS LATER. PROBE NO. 6 AND 8 WERE IMPLANTED INTO THE SAME ANIMAL, AT DIFFERENT STEREOTACTIC COORDINATES

Probe no.	Length [mm]	Width [ $\mu\text{m}$ ]	Thickness [ $\mu\text{m}$ ]	Electrode configuration	Tested at	Implantation target, in reference to the bregma [mm]
1	1,5	206	200	Linear	Lab A	AP: -4.0, ML: 3.0
2	1,5	400	200	Linear	Lab A	AP: -4.0, ML: 3.0
3	3	400	200	Tetrode	Lab A	AP: -4.0, ML: 3.0
4	3	400	380	Tetrode	Lab B	AP: -3.0, ML: 3.2
5	3	400	200	Linear	Lab B	AP: -3.0, ML: 3.2
6	3	400	200	Tetrode	Lab B	AP: -3.0, ML: 3.0
7	5	206	380	Tetrode	Lab B	AP: -3.0, ML: 3.0
8	7	400	200	Linear	Lab B	AP: -2.0, ML: 3.5

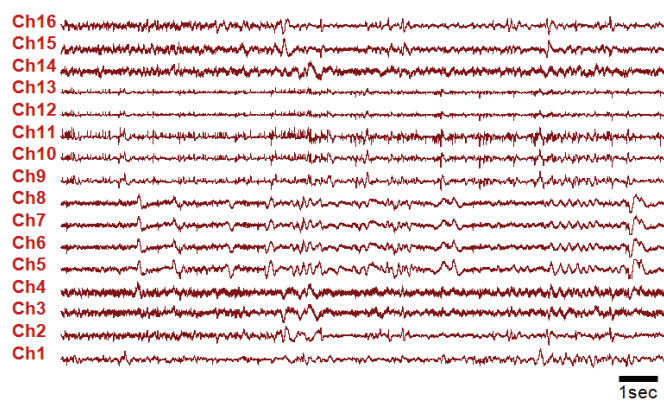


Fig. 4. Representative depth profiles of local field potentials patterns.

144 on the backside of the wafer used as a stopping layer during the subsequent deep-reactive ion etching of silicon. The 3D  
 145 micromachining process was performed in an Oxford Plasmalab System 100 chamber using Bosch process. Schematic  
 146 cross-sectional view of the probe during the fabrication process is shown on Fig. 2.C.  
 147  
 148  
 149

150 The probes have been flipped out of the wafer and glued  
 151 onto a printed circuit board (PCB) with a two-component  
 152 epoxy resin (Araldit AY103/HY956). 50  $\mu\text{m}$  thick Al wires  
 153 have been employed to establish connection between the bond-  
 154 ing pads and the PCB leads using a Kulicke-Soffa ultrasonic  
 155 wire bonder. For the insulation and protection of the Al wires,  
 156 the same resin has been used as for the gluing.

### 157 C. Methods of *in Vivo* Measurements

158 Functional tests of eight thus manufactured MEAs have  
 159 been performed in the cerebrum of anesthetized rats ( $n=3+4$ )  
 160 at two separate laboratories, the Laboratory of Proteomics,  
 161 Institute of Biology, Eötvös Loránd University (Lab A) and  
 162 the Comparative Psychophysiology Laboratory of the Insti-  
 163 tute of Cognitive Neuroscience and Psychology, RCNS-HAS  
 164 (Lab B). In both laboratories, animal care and experiments  
 165 were performed in compliance with order 243/1988 of the  
 166 Hungarian Government, which is an adaptation of directive

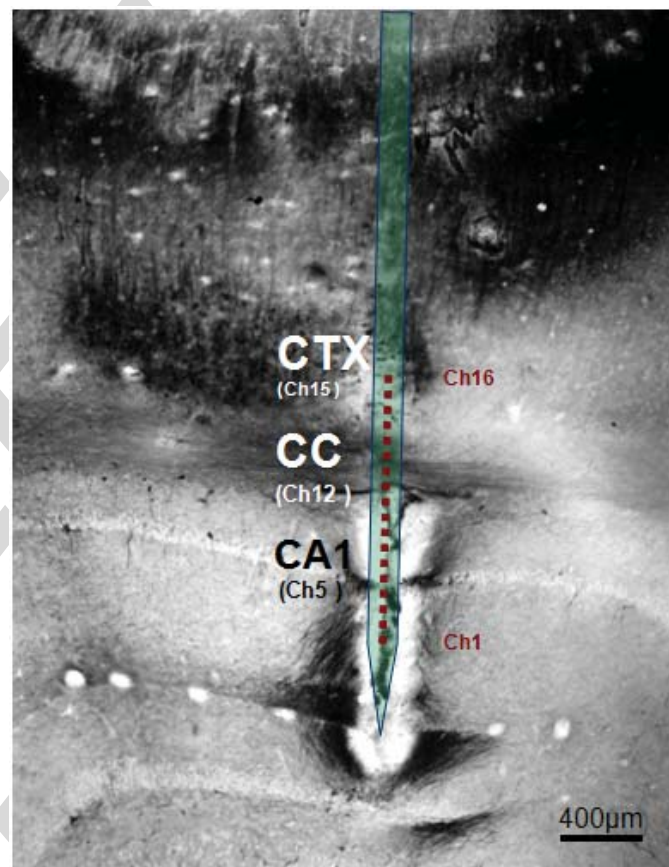


Fig. 5. Histological section showing silicon probe track. The sample has been stained with the Gallyas method.

86/609/EGK of the European Committee Council. Animals  
 have been anesthetized and submitted to stereotactic surgery,  
 targeting cortical, hippocampal and thalamic neural regions.  
 Table 1 summarizes the probes functionally tested *in vivo*.

At the Laboratory of Proteomics (Lab A), surgical pro-  
 cedures have been carried out as follows. Electrodes were  
 implanted in urethane anesthesia using Kopf stereotactic  
 instrument into the cerebrum of male Sprague–Dawley rats.  
 A midline cut was made in the scalp to expose the skull.

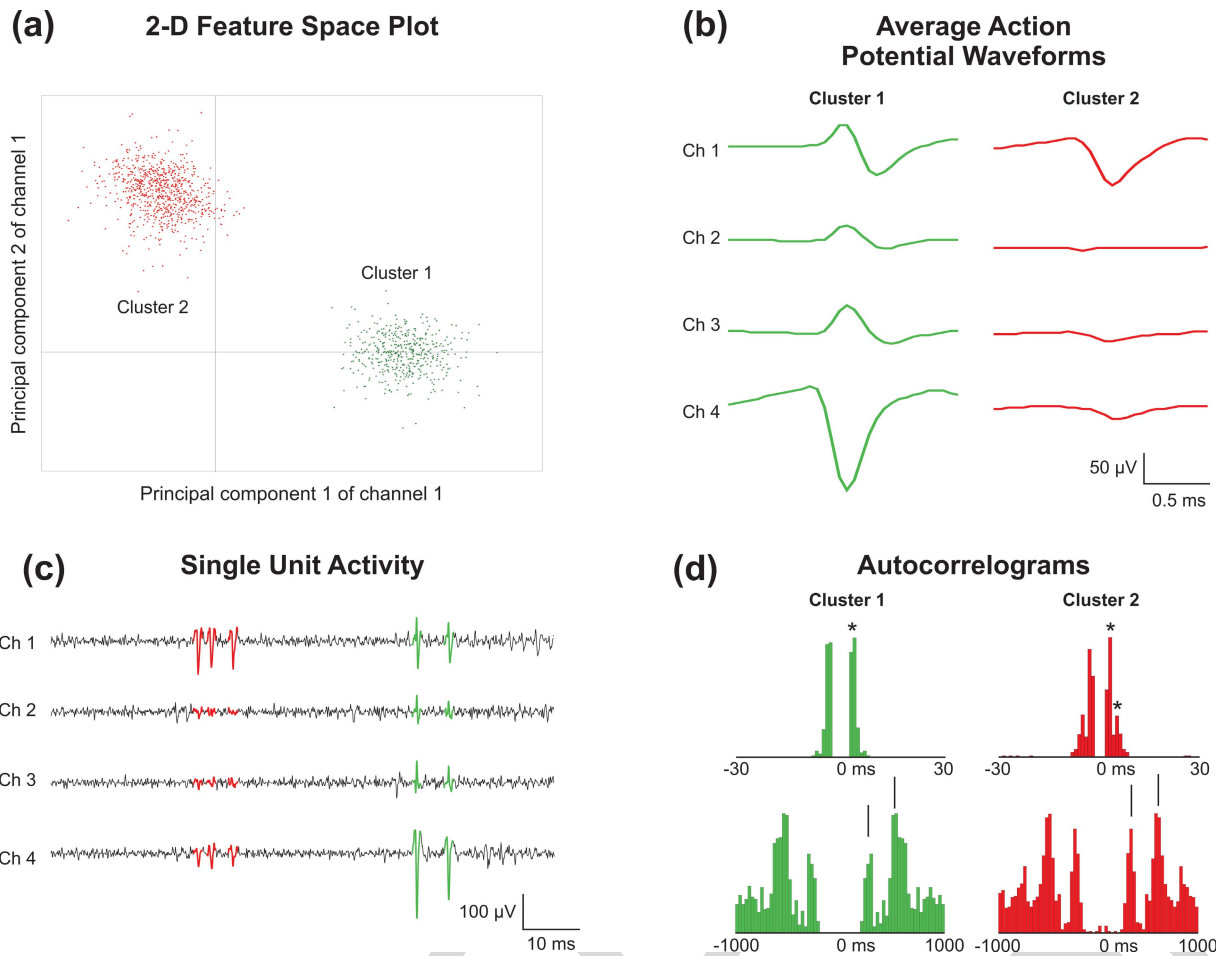


Fig. 6. The result of spike sorting performed on a tetrode recording from the thalamus (a) The 2-D feature space plot with two well separable single unit clusters (red and green cloud of dots). The selected features for spike sorting were the principal components of the spike waveforms. (b) Average action potential waveforms of the two separated unit clusters on different recording channels. Cluster 1 (green unit) has clearly visible action potentials on all four channels with different peak amplitudes. The size of spikes in cluster 2 (red unit) are the biggest on channel 1 and 4. (c) A 100 ms segment of a bandpass filtered (500-5000 Hz) unit activity recording with sample spikes of the two isolated clusters. The green unit was a bursting thalamocortical neuron with two action potentials per burst on average, whereas the other thalamic cell (red unit) fired mostly three spikes during one burst. (d) Autocorrelograms of the red and green clusters on two different timescales. The upper pictures show clear refractory periods (no spiking between 0–1 ms) in case of both of the clusters and several peaks (asterisks) between 2 and 5 ms that refer to the bursting nature of the thalamocortical neurons during anesthesia. The peaks (arrows) on the bottom autocorrelograms around 250 and 500 ms implies a strong correlation between the unit activity and the ongoing delta (2–4 Hz) and slow (0.5–2 Hz) oscillations which are the major brain rhythms in the thalamus during sleep and anesthesia.

176 A 2.0 mm diameter hole was drilled in the skull centered  
 177 4.0 mm posterior and 3.0 mm lateral from the bregma.  
 178 A 1.2 mm diameter screw was inserted into the skull above  
 179 the cerebellum on each side; these served as ground and  
 180 electrical reference. The dura exposed by the hole was cut  
 181 and the electrode tip was lowered 2.5–5.5 mm below the  
 182 brain surface. Spikes and EEG activity was separately recorded  
 183 from the same 16 channels (32 channel Neuralynx Cheetah  
 184 data Acquisition system, Neuralynx Inc., Tucson, AZ, USA)  
 185 with different filter settings. The extracellular action potentials  
 186 were captured at 30 kHz (amplification 50,000 $\times$ , filtering  
 187 300 Hz–6 kHz) and the local EEG were recorded continuously  
 188 at 5 kHz (amplification 10,000 $\times$ , filtering 1 Hz–475 Hz).  
 189 Probes were explanted and rats were sacrificed with a sodium  
 190 pentobarbital overdose and perfused transcardially with saline  
 191 followed by 4% paraformaldehyde (PFA) in phosphate buffer.  
 192 Brains were removed, stored in 4% PFA. Using a microtome,  
 193 60  $\mu$ m coronal sections were taken. For histological studies,

the slices were stained with the Gallyas silver method, a tool  
 for qualitative investigations on the presence of injured  
 neurons [16].

At the Comparative Psychophysiology Laboratory (Lab B),  
 four Wistar rats were used for the experiments. Initial anes-  
 thesia was administered via intraperitoneal injection of a  
 mixture of 37.5 mg/ml ketamine and 5 mg/ml xylazine at  
 0.2 ml/100 g body weight injection volume. The body tem-  
 perature was maintained at 37  $^{\circ}$ C with an electric heat-  
 ing pad. Animals were mounted in a stereotaxic frame  
 (David Kopf) and a 3 $\times$ 3 mm craniotomy was drilled in  
 the skull above the trunk region of the somatosensory cor-  
 tex (S1Tr) [22]. The deep anesthesia was maintained with  
 subsequent intramuscularly injected ketamine-xylazine doses  
 (0.2 ml/h). The probe attached to the micromanipulator was  
 slowly inserted into the cerebrum of the animal without  
 removing the dura mater. Stereotactic coordinates of the targets  
 are presented in table 1. The brain surface was bathed in

194  
 195  
 196  
 197  
 198  
 199  
 200  
 201  
 202  
 203  
 204  
 205  
 206  
 207  
 208  
 209  
 210  
 211

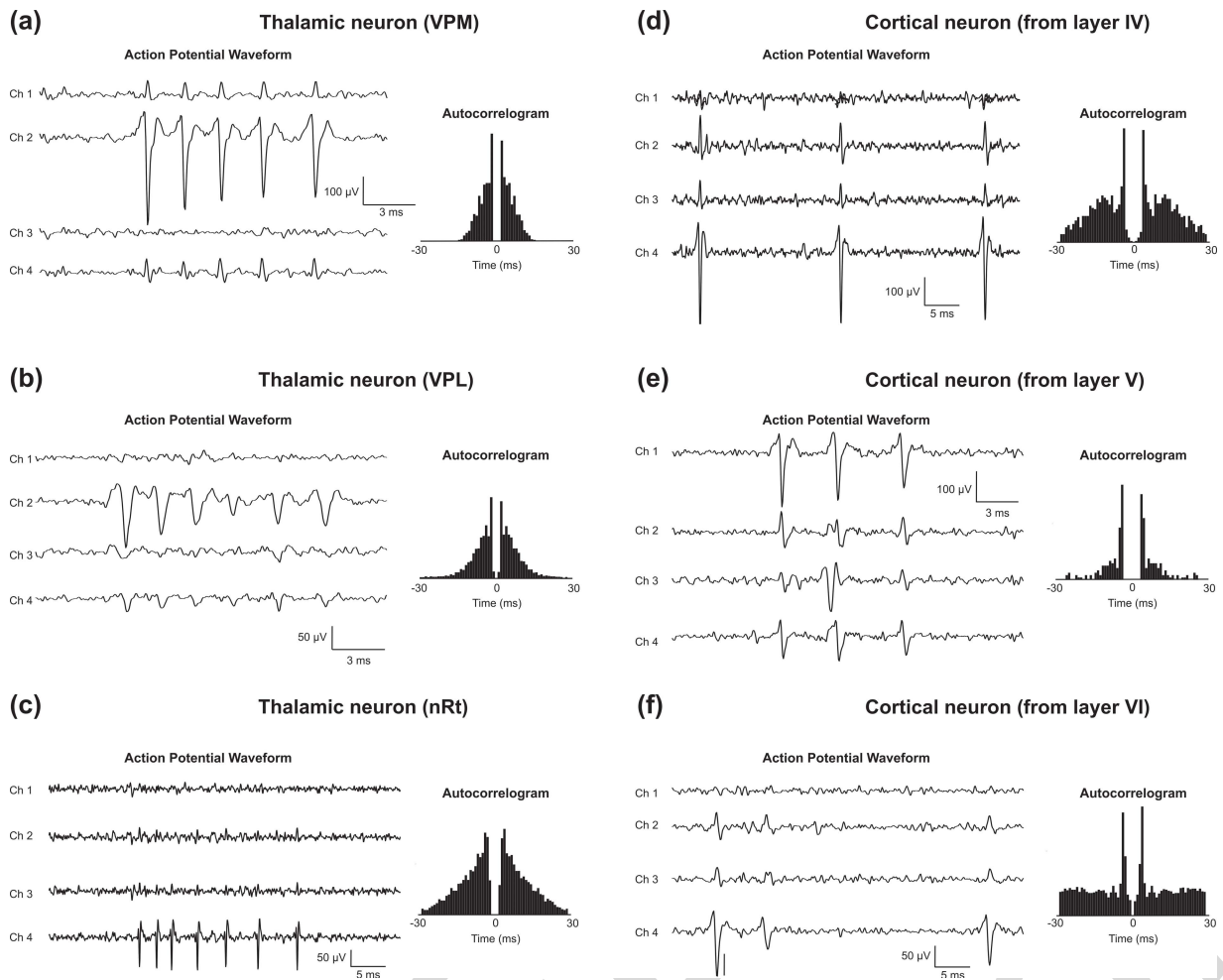


Fig. 7. Representative samples of the spike waveforms (left) and corresponding autocorrelograms (right) recorded with the silicon tetrode from the thalamus and cortex during anesthesia (a)–(f) Peak-to-peak action potential amplitudes ranged from a few dozen microvolts up to 400 microvolts (a) and the spikes of the same unit were in most cases clearly visible on more than one channel. Most of the sorted neurons were bursting cells with 2–6 spikes per burst.

212 saline to prevent it from drying. Wide bandwidth electrical  
 213 activity (0.1–7000 Hz) with a gain of 1000 was recorded with  
 214 20 kHz/channel sampling rate, at 16 bit precision with custom  
 215 made hardware and software and stored on a hard drive.  
 216 After the recording sessions the electrodes were withdrawn  
 217 and the animals were deeply anesthetized. The multiple unit  
 218 activity (MUA) and single unit activity (SUA) was extracted  
 219 from the raw wideband signals offline with a band-pass filter  
 220 (500–5000 Hz, 24 dB/oct, zeropaseshift) using NeuroScan  
 221 4.3 software (Compumedics, El Paso, TX). Spike sorting was  
 222 used to distinguish single from multiple unit activity. Units  
 223 were identified and isolated manually with a freely available  
 224 software (<http://www.klusters.sourceforge.net>) [23].

### 225 III. RESULTS AND DISCUSSION

#### 226 A. *In Vivo* Measurements – Overview

227 During stereotactic surgeries, all of the microelectrodes  
 228 presented in table 1 have proven to be robust enough for  
 229 acute use, since neither bending has occurred during implan-  
 230 tations, nor any sign of damage could be observed after  
 231 operations. Various, healthy local field potential (LFP) signals  
 232 were recorded with these probes. Using tetrodes, single unit

activities (spikes) were detected more frequently, as expected,  
 due to the smaller geometric area of their recording sites  
 [24], but spikes have also been recorded with linear probes.  
 In this paper, local field potential recordings and histological  
 studies are presented with a linear MEA (Probe no. 2), unit  
 activity detection and sorting is presented with a tetrode (probe  
 no. 6). The other 6 MEAs have also proven to be functionally  
 appropriate.

#### 241 B. *Local Field Potential Recording and Histology With a* 242 *Linear Probe*

243 In this section, measurements with probe no. 3 are presented  
 244 (its properties are listed in table 1.). Locations of the electrode  
 245 sites in the brain were first approximated from the recorded  
 246 waveforms (Fig. 5.). According to our observations, the probe  
 247 extended into the following anatomical structures.

- Cortex (CTX) - channel 15. 248
- Corpus callosum (CC) - channel 12. 249
- The Cornu Ammonis 1 region of the hippocampus (CA1)  
 - channel 5. 250

251 Power spectral density calculations on the recorded signals  
 252 show that the activities were different on all 16 channels.  
 253

254 These results were in correlation with the histological find- 309  
 255 ings carried out afterwards. With slicing, the tissue including 310  
 256 the probe track has been successfully explored. Gallyas stain- 311  
 257 ing procedure was employed in order to reveal injured cells 312  
 258 around the implantation site (Fig. 6.). The procedure has been 313  
 259 only used for visualization, not for quantitative analysis of 314  
 260 cell loss. 315

### 261 C. Spike Detection and Sorting With a Tetrode

262 Good quality single and multiple unit activity were recorded 316  
 263 from the cortex and thalamus with probe no. 6. A total of 317  
 264 35 cells were recorded from the cortical and thalamic areas 318  
 265 (cortex,  $n = 13$ ; thalamus,  $n = 22$ ) and two or three clusters 319  
 266 could be separated in general from the recorded unit activity  
 267 at one recording position (Fig. 6.). The mean peak-to-peak  
 268 amplitude of the averaged action potentials of the cells was  
 269  $128.9 \pm 54.3 \mu\text{V}$  (range:  $43.6 - 244.5 \mu\text{V}$ ) and the number  
 270 of spikes in a sorted unit cluster was  $1452 \pm 1829$  on average  
 271 (range: 47-9433). Clusters clearly separated on one plane  
 272 of the feature space (first three principal components) were  
 273 selected as putative neurons. Clear refractory periods (1-2 ms)  
 274 visible on the autocorrelograms of the separated clusters were  
 275 signs of appropriate spike sorting. In most cases the action  
 276 potential waveforms of the same unit could be detected on  
 277 several of the four channels simultaneously (Fig 6.). We also  
 278 calculated the distribution of the channels where the largest  
 279 negative peak of the spikes of the recorded neurons was  
 280 detected, but found no significant differences between the  
 281 channels (Channel 1: 8 units, 22.9 %; Channel 2: 12 units,  
 282 34.3 %, Channel 3: 5 units, 14.3 %; Channel 4: 10 units,  
 283 28.5 %). These results indicate that the spatial position of the  
 284 tetrode contacts had no effect on the action potential recording  
 285 capabilities of the probe.

286 The majority of the neurons were excitatory pyramidal 320  
 287 cells ( $n = 13$ ) and thalamocortical cells ( $n = 21$ ) with 321  
 288 wide spikes (half-amplitude duration:  $319 \pm 69.4 \mu\text{s}$ , range: 322  
 289  $208.5 - 452 \mu\text{s}$ ), except for one neuron with narrow action 323  
 290 potentials ( $164.5 \mu\text{s}$ ) recorded from the nucleus reticularis 324  
 291 thalami (nRt, Fig 7. (c)). The nRt consists of GABAergic 325  
 292 inhibitory cells that sends their axon collaterals to several "first 326  
 293 order" and "higher order" thalamic nuclei. Representative 327  
 294 spike waveforms of neurons recorded from different thalamic 328  
 295 nuclei and cortical layers are shown in Fig. 7. Bursting neurons 329  
 296 with 2-6 spikes in one burst event are typical to the somatosen- 330  
 297 sory nuclei (VPL, VPM, Po, Fig 7. (a)-(b)) of the thalamus 331  
 298 during anesthesia. The nRt neuron fired bursts containing 332  
 299 6-10 action potentials (Fig 7. (c)), while the recorded cortical 333  
 300 cells discharged mostly single spikes, spike doublets or triplets 334  
 301 (Fig. 7. (d)-(f)). During deep sleep and anesthesia brain 335  
 302 rhythms with lower frequencies (slow oscillation, 0.5-2 Hz; 336  
 303 delta, 2-4 Hz [25]), can be recorded from the thalamus and 337  
 304 cortex and the neuron discharges are time locked to the active 338  
 305 phases of these oscillations (Fig. x. (d)).

## 306 IV. CONCLUSION

307 *In vivo* electrophysiological measurements on rats with 340  
 308 silicon-based neural multielectrode arrays with extreme length,

robust mechanical parameters and adequate implantation and 309  
 targeting capabilities were performed in two separate labo- 310  
 ratories. Successful functional tests and histological studies 311  
 suggest that even though the probes presented here are thicker 312  
 and wider than commonly used silicon-based devices, they are 313  
 suitable for obtaining electronic interface with the cerebrum 314  
 of a small rodent. We suppose that since these probes are 315  
 of superior length, they are suitable candidates for acute *in* 316  
*vivo* experiences on animals with larger brain, such as cats or 317  
 primates, although further tests are necessary to ascertain this 318  
 assumption. 319

## V. ACKNOWLEDGEMENT

We are grateful to Mrs. Károlyné Payer, Mr. András 321  
 Straszner, Mr. Róbert Hodován and Mr. András Lőrincz for 322  
 their support in the clean room. We also wish to thank 323  
 Mr. Attila Nagy and Mr. István Réti for their help in chip 324  
 packaging. Useful and motivating discussions with Dr. László 325  
 Grand are greatly acknowledged. 326

## REFERENCES

- [1] J. S. Perlmutter and J. W. Mink, "Deep brain stimulation," *Annu. Rev. Neurosci.*, vol. 29, pp. 229-257, Aug. 2006. 328
- [2] D. M. Taylor, S. I. Tillery, and A. B. Schwartz, "Direct cortical control of 3D neuroprosthetic devices," *Science*, vol. 296, no. 5574, pp. 1829-1832, Apr. 2002. 329
- [3] F. H. Guenther, J. S. Brumberg, E. J. Wright, A. Nieto-Castanon, J. A. Tourville, M. Panko, R. Law, S. A. Siebert, J. L. Bartels, D. S. Andreasen, P. Ehirim, H. Mao, and P. R. Kennedy, "A wireless brain-machine interface for real-time speech synthesis," *PLoS ONE*, vol. 4, no. 12, p. e8218, Dec. 2009. 330
- [4] G. Kotzar, M. Freas, P. Abel, A. Fleischman, S. Roy, C. Zorman, J. M. Moran, and J. Melzak, "Evaluation of MEMS materials of construction for implantable medical devices," *Biomaterials*, vol. 23, no. 13, pp. 2737-2750, Jul. 2002. 331
- [5] A. Bragin, J. Hetke, C. L. Wilson, D. J. Anderson, J. Engel, Jr., and G. Buzsáki, "Multiple site silicon-based probes for chronic recordings in freely moving rats: Implantation, recording and histological verification," *J. Neurosci. Methods*, vol. 98, no. 1, pp. 77-82, May 2000. 332
- [6] P. J. Rousche and R. A. Normann, "Chronic recording capability of the Utah Intracortical Electrode Array in cat sensory cortex," *J. Neurosci. Methods*, vol. 82, no. 1, pp. 1-15, Jul. 1998. 333
- [7] K. Torab, T. S. Davis, D. J. Warren, P. A. House, R. A. Normann, and B. Greger, "Multiple factors may influence the performance of a visual prosthesis based on intracortical microstimulation: Nonhuman primate behavioural experimentation," *J. Neural Eng.*, vol. 8, no. 3, pp. 035001-1-035001-18, Jun. 2011. 334
- [8] M. Hajji-Hassan, V. P. Chodavarapu, and S. Musallam, "Microfabrication of ultra-long reinforced silicon neural electrodes," *IET Micro Nano Lett.*, vol. 4, no. 1, pp. 53-58, Mar. 2009. 335
- [9] D. T. Kewley, M. D. Hills, D. A. Borkholder, I. E. Opris, N. I. Maluf, C. W. Stormont, J. M. Bower, and G. T. A. Kovacs, "Plasma-etched neural probes," *Sens. Actuators A, Phys.*, vol. 58, no. 1, pp. 27-35, Jan. 1997. 336
- [10] P. J. Rousche, D. S. Pellinen, D. P. Pivin, Jr., J. C. Williams, R. J. Vetter, and D. R. Kirke, "Flexible polyimide-based intracortical electrode arrays with bioactive capability," *IEEE Trans. Biomed. Eng.*, vol. 48, no. 3, pp. 361-371, Mar. 2001. 337
- [11] A. Mercanzini, K. Cheung, D. L. Buhl, M. Boers, A. Maillard, P. Colin, J. C. Bensadoun, A. Bertsch, and P. Renaud, "Demonstration of cortical recording using novel flexible polymer neural probes," *Sens. Actuators A, Phys.*, vol. 143, no. 1, pp. 90-96, 2008. 338
- [12] V. S. Polikov, P. A. Tresco, and W. M. Reichert, "Response of brain tissue to chronically implanted neural electrodes," *J. Neurosci. Methods*, vol. 148, no. 1, pp. 1-18, Oct. 2005. 339
- [13] A. A. Fomani, M. Moradi, S. Assaf, and R. R. Mansour, "3D micro-probes for deep brain stimulation and recording," in *Proc. Annu. Int. Conf. IEEE Eng. Med. Biol. Soc.*, Sep. 2010, pp. 1808-1811. 340

- [14] S. Felix, K. Shah, D. George, V. Tolosa, A. Tooker, H. Sheth, T. Delima, and S. Pannu, "Removable silicon insertion stiffeners for neural probes using polyethylene glycol as a biodegradable adhesive," in *Proc. Annu. Int. Conf. IEEE Eng. Med. Biol. Soc.*, Aug. 2012, pp. 871–874.
- [15] D. Lewitus, K. L. Smith, W. Shain, and J. Kohn, "Ultrafast resorbable polymers for use as carriers for cortical neural probes," *Acta Biomater.*, vol. 7, no. 6, pp. 2483–2491, Jun. 2011.
- [16] F. Gallyas, M. Hsu, and G. Buzsáki, "Four modified silver methods for thick sections of formaldehyde-fixed mammalian central nervous tissue: 'Dark' neurons, perikarya of all neurons, microglial cells and capillaries," *J. Neurosci. Methods*, vol. 50, no. 2, pp. 159–64, Nov. 1993.
- [17] M. Welkenhuysen, A. Andrei, L. Ameye, W. Eberle, and B. Nuttin, "Effect of insertion speed on tissue response and insertion mechanics of a chronically implanted silicon-based neural probe," *IEEE Trans. Biomed. Eng.*, vol. 58, no. 11, pp. 3250–3259, Nov. 2011.
- [18] K. Najafi and J. F. Hetke, "Strength characterization of silicon microprobes in neurophysiological tissues," *IEEE Trans. Biomed. Eng.*, vol. 37, no. 5, pp. 474–481, May 1990.
- [19] Z. Fekete, Z. Hajnal, G. Márton, P. Fürjes, and A. Pongrácz, "Fracture analysis of silicon microprobes designed for deep-brain stimulation," *Microelectron. Eng.*, vol. 103, pp. 160–166, Mar. 2013.
- [20] A. M. Dymond, L. E. Kaechele, J. M. Jurist, and P. H. Crandall, "Brain tissue reaction to some chronically implanted metals," *J. Neurosurg.*, vol. 33, no. 5, pp. 574–580, Nov. 1970.
- [21] D. R. Merrill, M. Bikson, and J. G. Jefferys, "Electrical stimulation of excitable tissue: Design of efficacious and safe protocols," *J. Neurosci. Methods*, vol. 141, no. 2, pp. 171–198, Feb. 2005.
- [22] G. Paxinos and C. Watson, *The Rat Brain in Stereotaxic Coordinates, Compact Sixth Edition*. San Diego, CA, USA: Academic, 2009.
- [23] L. Hazan, M. Zugaro, and G. Buzsáki, "Klusters, neuroscope, NDmanager: A free software suite for neurophysiological data processing and visualization," *J. Neurosci. Methods*, vol. 155, no. 2, pp. 207–216, Sep. 2006.
- [24] M. A. Moffitt and C. C. McIntyre, "Model-based analysis of cortical recording with silicon microelectrodes," *Clinical Neurophysiol.*, vol. 116, no. 9, pp. 2240–2250, Sep. 2005.
- [25] M. Steriade, "The corticothalamic system in sleep," *Frontiers Biosci.*, vol. 8, no. 1, pp. 878–899, 2003.

**Gergely Márton** received the M.Sc. degree in electrical engineering from the Budapest University of Technology and Economics, Műegyetem rakpart, Hungary, in 2010.

He is currently pursuing the Ph.D. degree with the János Szentágothai Doctoral School of Neuroscience, Semmelweis University, Budapest, Hungary, and is a Research Assistant with the Institute of Cognitive Neuroscience and Psychology, Research Centre for Natural Sciences, Hungarian Academy of Sciences, Budapest. His current research interests include development of neural interfaces with MEMS technologies.

**Zoltán Fekete** received the M.Sc. and Ph.D. degrees in electrical engineering from the Budapest University of Technology and Economics, Budapest, Hungary, in 2009 and 2013, respectively.

He is currently a Research Fellow with the Research Institute of Technical Physics and Material Science, Hungarian Academy of Sciences, Budapest. His current research interests include the development of MEMS devices, silicon and polymer microfluidics, and silicon-based neural microprobes.

**Richárd Fiáth** received the M.Sc. degree in electrical and computer engineering from the Faculty of Information Technology, Peter Pazmany Catholic University, Budapest, Hungary, in 2009.

He is currently pursuing the Ph.D. degree with the János Szentágothai Doctoral School of Neuroscience, Semmelweis University, Budapest, and is a Research Assistant with the Institute of Cognitive Neuroscience and Psychology, Research Centre for Natural Sciences, Hungarian Academy of Sciences, Budapest. His current research interests include silicon-based neural interfaces, investigation of thalamocortical interactions, and the physiology of sleep.

**Péter Baracska** received the M.S. degree in neurobiology from Eötvös Lóránd University, Budapest, Hungary, in 2007.

He was a Research Assistant with the Department of Medical Chemistry, University of Szeged, Szeged, Hungary, from 2010 to 2011. He is currently with the Bay Zoltan Nonprofit Ltd. for Applied Research, Budapest, and is currently a Graduate Student with the Institute of Biology, Eötvös Lóránd University, Egyetem tér, Hungary.

**István Ulbert** received the M.Sc. degree in technological physics from the Technical University of Budapest, Budapest, Hungary, in 1988, the M.D. degree from the Medical School, Semmelweis University, Budapest, in 1997, and the Ph.D. degree in neurosciences from the Doctoral School, Semmelweis University, in 2002.

He gained scientific experience as a Research Associate with the Albert Einstein College of Medicine, Department of Neuroscience, Bronx, NY, USA, from 1994 to 1996, as a Post-Doctoral Fellow with Stanford University Medical School, Department of Neurosurgery, Stanford, CA, USA, from 1997 to 2000, and as an Instructor of radiology with Harvard University Medical School, Department of Radiology, Massachusetts General Hospital, Boston, MA, USA, from 2000 to 2003. He is currently a Senior Research Scientist and a Group Leader with the Institute of Cognitive Neuroscience and Psychology, Research Centre for Natural Sciences, Hungarian Academy of Sciences, Budapest, and an Associate Professor with the Faculty of Information Technology, Pázmány Péter Catholic University, Budapest. He has co-authored over 50 articles in peer-reviewed journals and over 250 publications in the forms of conference proceedings, book chapters, posters, and lectures. His current research interests include the development of implantable cortical biosensors for human and animal applications and the investigation of intracortical generators of brain oscillations.

**Gábor Juhász**, photograph and biography are not available at the time of publication.

**Gábor Battistig**, photograph and biography are not available at the time of publication.

**Anita Pongrácz** received the M.Sc. degree in engineering physics from the Technical University of Budapest, Budapest, Hungary, in 2004.

She was a Baseline Process Engineer with the University of California, Berkeley Microfabrication Laboratory, Berkeley, CA, USA, from 2006 to 2007. Her main responsibilities were to design, fabricate, test, and evaluate CMOS test devices. She received the Ph.D. degree in 2010 and is currently a Research Fellow with the Institute of Technical Physics and Material Science, Hungarian Academy of Sciences, Budapest. Her current research interests include microfabrication of neuroMEMS devices.

429

430

431

432

433

434

435

436

437

438

439

440

441

442

443

444

445

446

447

448

449

450

451

452

453

454

455

456

457

458

459

460

461

462

463

464

465

466

467

468

469

470

471

472

473

474

475

476

477

478

479

480

481

482

483

484

485

486

487

488

489

490

491

492

493

494

495

496

497

498

499

500

501

502

503

504

505

506

507

508

509

510

511

512

## AUTHOR QUERIES

- AQ:1 = Images 1, 3, and 4 are not cited in the text. Please indicate where they should be cited.
- AQ:2 = Please confirm whether “kirke” is “Kirke” or “Kipke.”
- AQ:3 = Please provide biography for the authors “Gábor Juhász and Gábor Battistig” if desired.

IEEE  
Proof

# *In Vivo* Measurements With Robust Silicon-Based Multielectrode Arrays With Extreme Shaft Lengths

Gergely Márton, Zoltán Fekete, Richárd Fiáth, Péter Baracskaý, István Ulbert, Gábor Juhász, Gábor Battistig, and Anita Pongrácz

**Abstract**—In this paper, manufacturing and *in vivo* testing of extreme-long Si-based neural microelectrode arrays are presented. Probes with different shaft lengths (15–70 mm) are formed by deep reactive ion etching and have been equipped with platinum electrodes of various configurations. *In vivo* measurements on rats indicate good mechanical stability, robust implantation, and targeting capability. High-quality signals have been recorded from different locations of the cerebrum of the rodents. The accompanied tissue damage is characterized by histology.

**Index Terms**—Neural microelectrode array, deep-brain electrode, silicon-based microelectromechanical system, spike sorting.

## I. INTRODUCTION

ELECTRODES, implanted into the central nervous system (CNS) are gaining increasing attention as they are being applied on a widening scale for medical purposes. With deep-brain stimulation, patients with Parkinson’s disease or essential tremor can be treated [1], while cortical implants have been employed for control of prosthetic devices [2] and speech restoration [3].

In order to create electronic interfaces with the CNS, silicon-based microstructures are suitable candidates, since they can be provided with widely variable electrode configurations in a precise and reproducible manner, using highly biocompatible materials [4]. These devices allow good quality local field potential, single and multiple unit activity recordings [5], therefore they are frequently applied in experimental neurophysiology as well *in vivo*, in the CNS of small mammals,

Manuscript received December 12, 2012; revised April 9, 2013; accepted April 24, 2013. The work of A. Pongrácz was supported by the Bolyai János Grant of HAS. The work of I. Ulbert was supported by the French-Hungarian Grant TAMOP-4.2.1.B-11/2/KMR-2011-0002. This work was supported by the Hungarian Science Foundation under Grant OTKA K81354, and by the French-Hungarian Grants ANR-TÉT Neurogen and ANRTÉT Multisca. The associate editor coordinating the review of this paper and approving it for publication was Prof. Aime Lay-Ekuakille.

G. Márton, Z. Fekete, R. Fiáth, I. Ulbert, G. Battistig, and A. Pongrácz are with the Hungarian Academy of Sciences, Budapest 240050, Hungary (e-mail: marton.gergely@tk.mta.hu; feketem@mfa.kfki.hu; fiath.richard@gmail.com; ulbert@cogpsyphy.hu; battisti@mfa.kfki.hu; pongracz.anita@tk.mta.hu).

P. Baracskaý is with the Department of Biology, Eötvös Loránd University, Budapest H-1117, Hungary, and also with the Bay Zoltan Nonprofit Ltd. for Applied Research, Budapest H-1116, Hungary (e-mail: baracskaý@gmail.com).

G. Juhász is with the Department of Biology, Eötvös Loránd University, Budapest H-1117, Hungary (e-mail: gjuhasz@dec001.geobio.elte.hu).

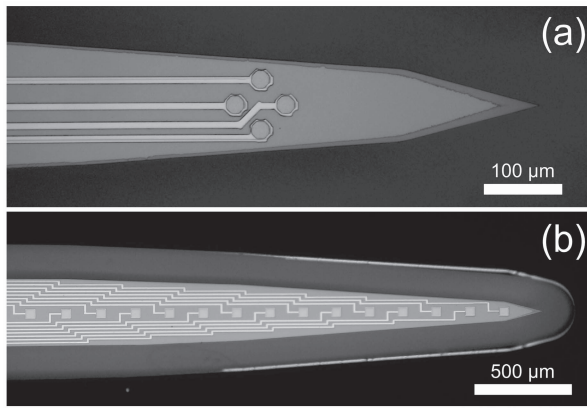
Color versions of one or more of the figures in this paper are available online at <http://ieeexplore.ieee.org>.

Digital Object Identifier 10.1109/JSEN.2013.2260325

e.g. rodents. During experiments performed on mammals with larger brain, such as cats [6] or primates [7], silicon-based microelectrode arrays (MEAs) are typically implanted close to the brain surface, into the cerebral cortex. The application of such probes to access brain regions located more than 1 cm below the brain surface is highly unusual. For this purpose reinforced silicon-based probes of 1.05 cm have been presented [8]. In order to interface neural structures located deeper, wire electrodes are more frequently used, as their mechanical robustness is superior to silicon-based devices. However, they lack the benefits of multielectrodes manufactured with microelectromechanical system (MEMS) technology, such as precise, reproducible location of custom-designed electrodes with microscale dimension and good integration capabilities [9].

Polymer-based implantable neural electrode arrays, manufactured with MEMS technology, have also been reported [10], [11]. These flexible devices are able to provide smoother coupling with the neural tissue than silicon. They can adapt to the motions of the brain, thus they cause a less intense immune response and glial scar formation around the probe [12]. However, obtaining precise targeting during penetration into deep-brain regions is difficult or impossible without a more robust support structure [13] or a method that stiffens the implant at least during insertion [14], [15]. Acute experiments are not so sensitive for tissue response like chronic experiments, while easy, precise targeting is an important factor in both cases. These considerations brought the development of silicon-based, deep-brain multielectrode arrays for acute use into our attention.

In this work, we investigated whether the length of functionally appropriate silicon-based MEAs, manufactured using standard MEMS technology can be increased to a much greater scale. Extending shaft thickness and/or width can be a way for providing sufficient mechanical robustness for the implants, but increasing cross-sectional dimensions also increases invasiveness. In order to investigate the functionality of a probe with unusually large dimensions, we have performed *in vivo* experiments on rat cortex, hippocampus and thalamus. Although the access of these anatomical regions would not require such long shafts, we expect them to be very appropriate targets in order to find out whether these probes cause severe tissue damage, e.g. excessive loss of the nearby neurons. We have performed extracellular recordings in the targeted regions and employed a staining procedure, suitable for indication of damaged cells [16].



AQ:1

Fig. 1. (a) Tetrode and (b) linear electrode array configurations.

## II. MATERIALS AND METHODS

### A. Probe Design

Studies on the factors affecting mechanical properties of silicon-based neural implants have been published [17], [18]. We intended to manufacture stiff, rather than flexible, single-shaft probes, suitable for the penetration of the meninges (including the dura mater) and precise targeting. Shaft thicknesses were defined by the substrate silicon wafers (200  $\mu\text{m}$  and 380  $\mu\text{m}$ ), while their widths and lengths could be freely varied: 206  $\mu\text{m}$  and 400  $\mu\text{m}$  wide shafts with four different lengths (15 mm, 30 mm, 50 mm and 70 mm) were designed. These parameters have been thoroughly combined. Preliminary study of mechanical characterization of bare silicon probes (without electrodes) of such geometries has been previously presented by our group [19].

The recording electrodes (sites) on the probe tip were arranged as tetrodes (4 electrodes per probe in rhombus vertices) and linear arrays (12 or 16 sites in the midline of the front side of the shaft). Considering the latter, center-to-center distances of the 30  $\mu\text{m}$   $\times$  30  $\mu\text{m}$  and 50  $\mu\text{m}$   $\times$  50  $\mu\text{m}$  recording areas were 100  $\mu\text{m}$  and 200  $\mu\text{m}$ , respectively. Tetrodes were optimized for measuring single-unit activities, thus they were more compactly designed: the octagonal sites, 22  $\mu\text{m}$  in diagonal, were located 46  $\mu\text{m}$  distant from each other. We have formed electrode sites of platinum, which is a commonly used noble metal in this field, because of its biostability [20], [21].

### B. Microfabrication and Packaging

The fabrication technology of the deep brain multielectrodes is based on a single-side, three mask bulk micromachining process sequence that proceeded in three phases. The overall process flow is summarized in Fig 2. 200  $\mu\text{m}$  and 400  $\mu\text{m}$  thick, double-side polished (100) oriented 4-inch silicon wafers were used for the probe fabrication. The initial phase consisted of thin-film depositions to form the bottom insulating layers, the electrodes and output leads (Fig. 2.A). In the second phase the upper passivation layers were deposited and the contact holes, bonding pads and contour of the probe body were formed by different etching steps (Fig. 2.B). In the last phase deep reactive ion etching (DRIE) was used to define the

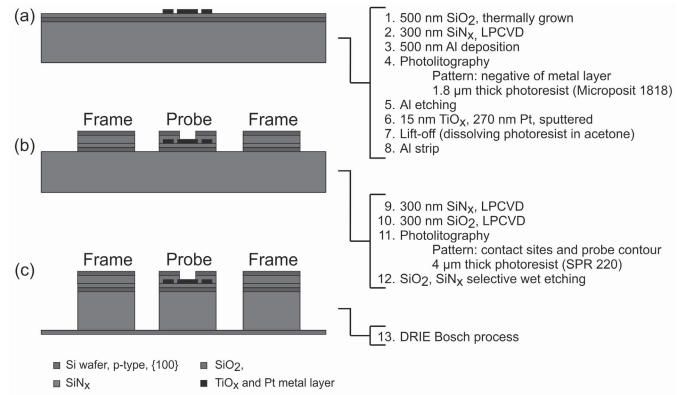


Fig. 2. Technological processes Forming lower insulator and patterned metal layers (a), upper insulator layers, opened at the sites (b), silicon dry etching with Bosch process (c).

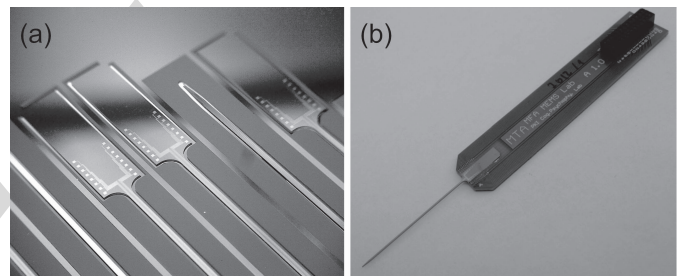


Fig. 3. (a) 16-channel multielectrodes on a micromachined silicon wafer. (b) A packaged silicon-based neural electrode on a PCB with shaft length of 3 cm.

probe shafts and bases (Fig.2.C) followed by the removal of the different masking layers and packaging of the probe.

Contact formation was obtained as follows. In the first step 500 nm thick SiO<sub>2</sub> layer was thermally grown on both sides of the wafer, followed by a deposition of 300 nm thick low-pressure chemical vacuum deposited (LPCVD) low stress silicon-nitride. The metal layer was then deposited and patterned by lift-off process. The lift-off structure composed of 1.8  $\mu\text{m}$  thick photoresist (Microposit 1818) layer over patterned Al thin film of 500 nm. The metal layer consisted of a 15 nm thick adhesion layer of TiO<sub>x</sub> and Pt. TiO<sub>x</sub> was formed by reactive sputtering of Ti in O<sub>2</sub> (Ar/O<sub>2</sub> ratio was 80:20) atmosphere. In the same vacuum cycle 270 nm thick Pt was sputtered on top of TiO<sub>x</sub>. The lift-off was accomplished by dissolving the photoresist pattern in acetone, this process was optimized by using water-cooled substrate holder which diminished the resist distortion during TiO<sub>x</sub>/Pt sputtering. Subsequently, the removal of Al patterns in four component etching solution and low pressure chemical vapor deposition of 300+300 nm thick SiN<sub>x</sub>/SiO<sub>2</sub> insulating layer stack occurred. Contact holes through the insulating layers were created by selective wet etching processes. By these processing steps, Pt lines insulated by SiN<sub>x</sub>/SiO<sub>2</sub> layers and formation of Pt contacts have been carried out.

For probe shaping a 500 nm thick Al layer was deposited on the front side and patterned by photolithography using 4  $\mu\text{m}$  thick SPR220 photoresist. The body of the probe was defined by Al wet etching. SPR220 photoresist was spun also

TABLE I

THE MAIN PROPERTIES OF THE MEAs, WHICH HAVE BEEN FUNCTIONALLY TESTED *in vivo*. MEASUREMENTS PERFORMED WITH PROBE NO. 2 AND 6 ARE PRESENTED IN DETAILS LATER. PROBE NO. 6 AND 8 WERE IMPLANTED INTO THE SAME ANIMAL, AT DIFFERENT STEREOTACTIC COORDINATES

Probe no.	Length [mm]	Width [ $\mu\text{m}$ ]	Thickness [ $\mu\text{m}$ ]	Electrode configuration	Tested at	Implantation target, in reference to the bregma [mm]
1	1,5	206	200	Linear	Lab A	AP: -4.0, ML: 3.0
2	1,5	400	200	Linear	Lab A	AP: -4.0, ML: 3.0
3	3	400	200	Tetrode	Lab A	AP: -4.0, ML: 3.0
4	3	400	380	Tetrode	Lab B	AP: -3.0, ML: 3.2
5	3	400	200	Linear	Lab B	AP: -3.0, ML: 3.2
6	3	400	200	Tetrode	Lab B	AP: -3.0, ML: 3.0
7	5	206	380	Tetrode	Lab B	AP: -3.0, ML: 3.0
8	7	400	200	Linear	Lab B	AP: -2.0, ML: 3.5

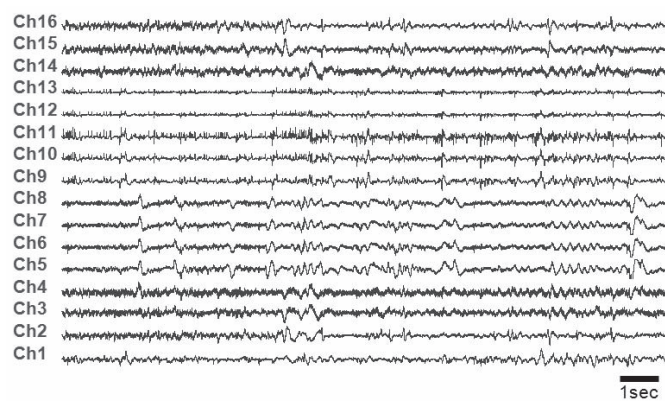


Fig. 4. Representative depth profiles of local field potentials patterns.

144 on the backside of the wafer used as a stopping layer during the subsequent deep-reactive ion etching of silicon. The 3D micromachining process was performed in an Oxford Plasmalab System 100 chamber using Bosch process. Schematic cross-sectional view of the probe during the fabrication process is shown on Fig. 2.C.

150 The probes have been flipped out of the wafer and glued onto a printed circuit board (PCB) with a two-component epoxy resin (Araldit AY103/HY956). 50  $\mu\text{m}$  thick Al wires have been employed to establish connection between the bonding pads and the PCB leads using a Kulicke-Soffa ultrasonic wire bonder. For the insulation and protection of the Al wires, the same resin has been used as for the gluing.

### 157 C. Methods of *in Vivo* Measurements

158 Functional tests of eight thus manufactured MEAs have been performed in the cerebrum of anesthetized rats ( $n=3+4$ ) at two separate laboratories, the Laboratory of Proteomics, Institute of Biology, Eötvös Loránd University (Lab A) and the Comparative Psychophysiology Laboratory of the Institute of Cognitive Neuroscience and Psychology, RCNS-HAS (Lab B). In both laboratories, animal care and experiments were performed in compliance with order 243/1988 of the Hungarian Government, which is an adaptation of directive

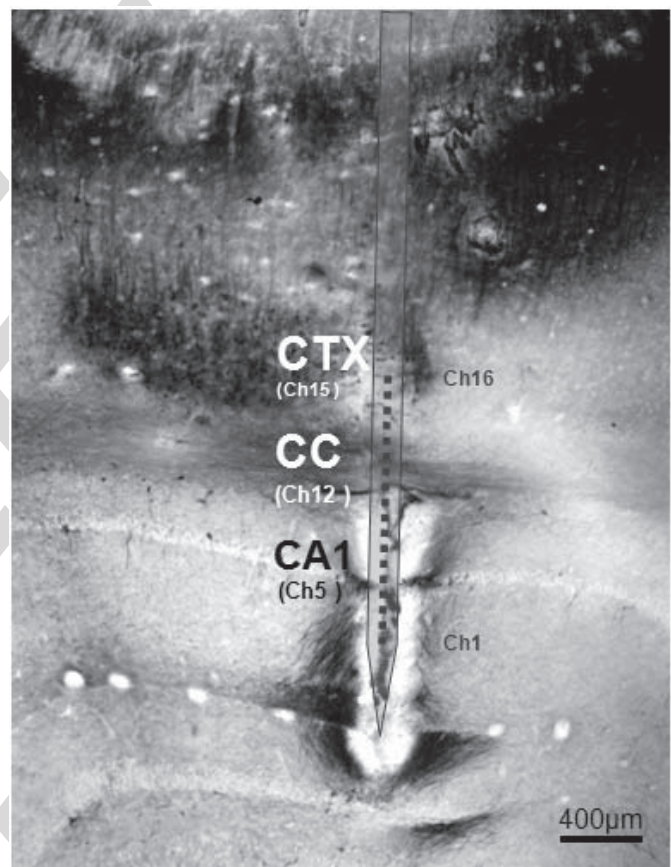


Fig. 5. Histological section showing silicon probe track. The sample has been stained with the Gallyas method.

167 86/609/EGK of the European Committee Council. Animals have been anesthetized and submitted to stereotactic surgery, targeting cortical, hippocampal and thalamic neural regions. Table 1 summarizes the probes functionally tested *in vivo*.

171 At the Laboratory of Proteomics (Lab A), surgical procedures have been carried out as follows. Electrodes were implanted in urethane anesthesia using Kopf stereotactic instrument into the cerebrum of male Sprague-Dawley rats. A midline cut was made in the scalp to expose the skull.

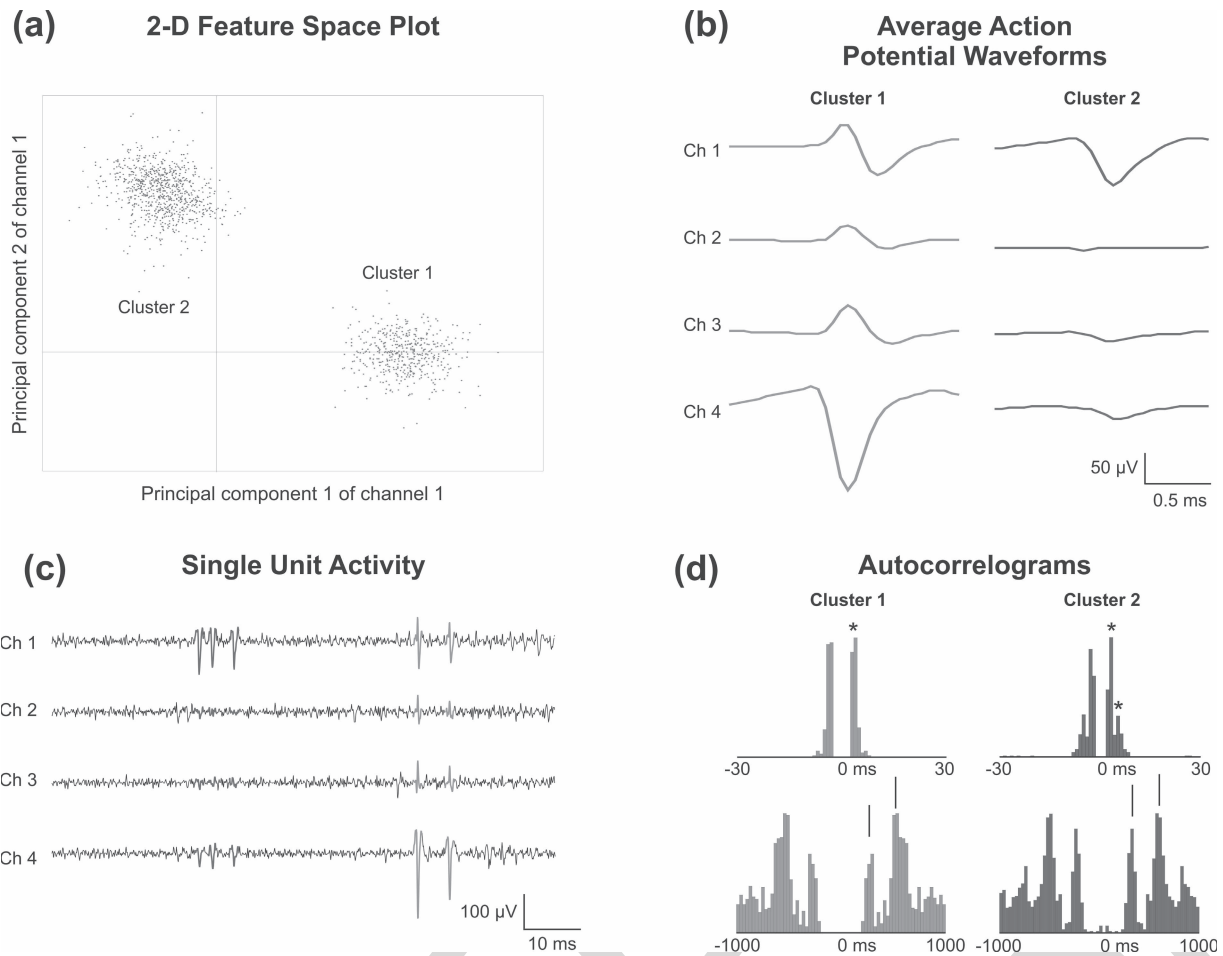


Fig. 6. The result of spike sorting performed on a tetrode recording from the thalamus (a) The 2-D feature space plot with two well separable single unit clusters (red and green cloud of dots). The selected features for spike sorting were the principal components of the spike waveforms. (b) Average action potential waveforms of the two separated unit clusters on different recording channels. Cluster 1 (green unit) has clearly visible action potentials on all four channels with different peak amplitudes. The size of spikes in cluster 2 (red unit) are the biggest on channel 1 and 4. (c) A 100 ms segment of a bandpass filtered (500-5000 Hz) unit activity recording with sample spikes of the two isolated clusters. The green unit was a bursting thalamocortical neuron with two action potentials per burst on average, whereas the other thalamic cell (red unit) fired mostly three spikes during one burst. (d) Autocorrelograms of the red and green clusters on two different timescales. The upper pictures show clear refractory periods (no spiking between 0–1 ms) in case of both of the clusters and several peaks (asterisks) between 2 and 5 ms that refer to the bursting nature of the thalamocortical neurons during anesthesia. The peaks (arrows) on the bottom autocorrelograms around 250 and 500 ms implies a strong correlation between the unit activity and the ongoing delta (2–4 Hz) and slow (0.5–2 Hz) oscillations which are the major brain rhythms in the thalamus during sleep and anesthesia.

176 A 2.0 mm diameter hole was drilled in the skull centered  
 177 4.0 mm posterior and 3.0 mm lateral from the bregma.  
 178 A 1.2 mm diameter screw was inserted into the skull above  
 179 the cerebellum on each side; these served as ground and  
 180 electrical reference. The dura exposed by the hole was cut  
 181 and the electrode tip was lowered 2.5–5.5 mm below the  
 182 brain surface. Spikes and EEG activity was separately recorded  
 183 from the same 16 channels (32 channel Neuralynx Cheetah  
 184 data Acquisition system, Neuralynx Inc., Tucson, AZ, USA)  
 185 with different filter settings. The extracellular action potentials  
 186 were captured at 30 kHz (amplification 50,000 $\times$ , filtering  
 187 300 Hz–6 kHz) and the local EEG were recorded continuously  
 188 at 5 kHz (amplification 10,000 $\times$ , filtering 1 Hz–475 Hz).  
 189 Probes were explanted and rats were sacrificed with a sodium  
 190 pentobarbital overdose and perfused transcardially with saline  
 191 followed by 4% paraformaldehyde (PFA) in phosphate buffer.  
 192 Brains were removed, stored in 4% PFA. Using a microtome,  
 193 60  $\mu$ m coronal sections were taken. For histological studies,

the slices were stained with the Gallyas silver method, a tool  
 for qualitative investigations on the presence of injured  
 neurons [16].

At the Comparative Psychophysiology Laboratory (Lab B),  
 four Wistar rats were used for the experiments. Initial anes-  
 thesia was administered via intraperitoneal injection of a  
 mixture of 37.5 mg/ml ketamine and 5 mg/ml xylazine at  
 0.2 ml/100 g body weight injection volume. The body tem-  
 perature was maintained at 37  $^{\circ}$ C with an electric heating  
 pad. Animals were mounted in a stereotaxic frame  
 (David Kopf) and a 3 $\times$ 3 mm craniotomy was drilled in  
 the skull above the trunk region of the somatosensory cor-  
 tex (S1Tr) [22]. The deep anesthesia was maintained with  
 subsequent intramuscularly injected ketamine-xylazine doses  
 (0.2 ml/h). The probe attached to the micromanipulator was  
 slowly inserted into the cerebrum of the animal without  
 removing the dura mater. Stereotactic coordinates of the targets  
 are presented in table 1. The brain surface was bathed in

194  
 195  
 196  
 197  
 198  
 199  
 200  
 201  
 202  
 203  
 204  
 205  
 206  
 207  
 208  
 209  
 210  
 211

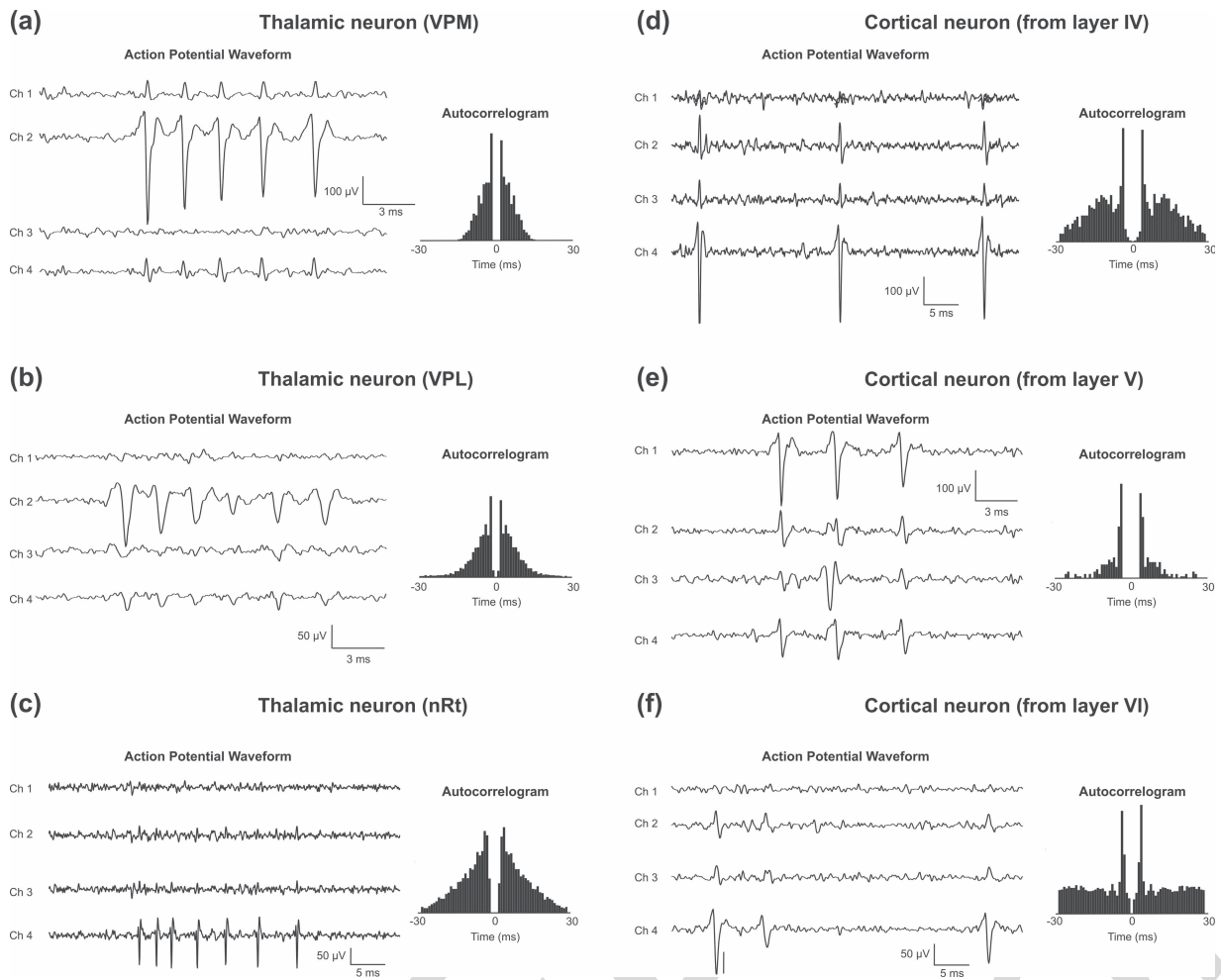


Fig. 7. Representative samples of the spike waveforms (left) and corresponding autocorrelograms (right) recorded with the silicon tetrode from the thalamus and cortex during anesthesia (a)–(f). Peak-to-peak action potential amplitudes ranged from a few dozen microvolts up to 400 microvolts (a) and the spikes of the same unit were in most cases clearly visible on more than one channel. Most of the sorted neurons were bursting cells with 2–6 spikes per burst.

212 saline to prevent it from drying. Wide bandwidth electrical  
 213 activity (0.1–7000 Hz) with a gain of 1000 was recorded with  
 214 20 kHz/channel sampling rate, at 16 bit precision with custom  
 215 made hardware and software and stored on a hard drive.  
 216 After the recording sessions the electrodes were withdrawn  
 217 and the animals were deeply anesthetized. The multiple unit  
 218 activity (MUA) and single unit activity (SUA) was extracted  
 219 from the raw wideband signals offline with a band-pass filter  
 220 (500–5000 Hz, 24 dB/oct, zeropaseshift) using NeuroScan  
 221 4.3 software (Compumedics, El Paso, TX). Spike sorting was  
 222 used to distinguish single from multiple unit activity. Units  
 223 were identified and isolated manually with a freely available  
 224 software (<http://www.klusters.sourceforge.net>) [23].

### 225 III. RESULTS AND DISCUSSION

#### 226 A. *In Vivo* Measurements – Overview

227 During stereotactic surgeries, all of the microelectrodes  
 228 presented in table 1 have proven to be robust enough for  
 229 acute use, since neither bending has occurred during implanta-  
 230 tions, nor any sign of damage could be observed after  
 231 operations. Various, healthy local field potential (LFP) signals  
 232 were recorded with these probes. Using tetrodes, single unit

activities (spikes) were detected more frequently, as expected,  
 due to the smaller geometric area of their recording sites  
 [24], but spikes have also been recorded with linear probes.  
 In this paper, local field potential recordings and histological  
 studies are presented with a linear MEA (Probe no. 2), unit  
 activity detection and sorting is presented with a tetrode (probe  
 no. 6). The other 6 MEAs have also proven to be functionally  
 appropriate.

#### 241 B. *Local Field Potential Recording and Histology With a* 242 *Linear Probe*

243 In this section, measurements with probe no. 3 are presented  
 244 (its properties are listed in table 1.). Locations of the electrode  
 245 sites in the brain were first approximated from the recorded  
 246 waveforms (Fig. 5.). According to our observations, the probe  
 247 extended into the following anatomical structures.

- Cortex (CTX) - channel 15. 248
- Corpus callosum (CC) - channel 12. 249
- The Cornu Ammonis 1 region of the hippocampus (CA1) 250
- channel 5. 251

Power spectral density calculations on the recorded signals  
 show that the activities were different on all 16 channels. 252  
 253

254 These results were in correlation with the histological find- 309  
 255 ings carried out afterwards. With slicing, the tissue including 310  
 256 the probe track has been successfully explored. Gallyas stain- 311  
 257 ing procedure was employed in order to reveal injured cells 312  
 258 around the implantation site (Fig. 6.). The procedure has been 313  
 259 only used for visualization, not for quantitative analysis of 314  
 260 cell loss. 315

### 261 C. Spike Detection and Sorting With a Tetrode

262 Good quality single and multiple unit activity were recorded 316  
 263 from the cortex and thalamus with probe no. 6. A total of 317  
 264 35 cells were recorded from the cortical and thalamic areas 318  
 265 (cortex,  $n = 13$ ; thalamus,  $n = 22$ ) and two or three clusters 319  
 266 could be separated in general from the recorded unit activity  
 267 at one recording position (Fig. 6.). The mean peak-to-peak  
 268 amplitude of the averaged action potentials of the cells was  
 269  $128.9 \pm 54.3 \mu\text{V}$  (range:  $43.6 - 244.5 \mu\text{V}$ ) and the number  
 270 of spikes in a sorted unit cluster was  $1452 \pm 1829$  on average  
 271 (range: 47-9433). Clusters clearly separated on one plane  
 272 of the feature space (first three principal components) were  
 273 selected as putative neurons. Clear refractory periods (1-2 ms)  
 274 visible on the autocorrelograms of the separated clusters were  
 275 signs of appropriate spike sorting. In most cases the action  
 276 potential waveforms of the same unit could be detected on  
 277 several of the four channels simultaneously (Fig 6.). We also  
 278 calculated the distribution of the channels where the largest  
 279 negative peak of the spikes of the recorded neurons was  
 280 detected, but found no significant differences between the  
 281 channels (Channel 1: 8 units, 22.9 %; Channel 2: 12 units,  
 282 34.3 %, Channel 3: 5 units, 14.3 %; Channel 4: 10 units,  
 283 28.5 %). These results indicate that the spatial position of the  
 284 tetrode contacts had no effect on the action potential recording  
 285 capabilities of the probe.

286 The majority of the neurons were excitatory pyramidal 320  
 287 cells ( $n = 13$ ) and thalamocortical cells ( $n = 21$ ) with 321  
 288 wide spikes (half-amplitude duration:  $319 \pm 69.4 \mu\text{s}$ , range: 322  
 289  $208.5 - 452 \mu\text{s}$ ), except for one neuron with narrow action 323  
 290 potentials ( $164.5 \mu\text{s}$ ) recorded from the nucleus reticularis 324  
 291 thalami (nRt, Fig 7. (c)). The nRt consists of GABAergic 325  
 292 inhibitory cells that sends their axon collaterals to several "first 326  
 293 order" and "higher order" thalamic nuclei. Representative 327  
 294 spike waveforms of neurons recorded from different thalamic 328  
 295 nuclei and cortical layers are shown in Fig. 7. Bursting neurons 329  
 296 with 2-6 spikes in one burst event are typical to the somatosen- 330  
 297 sory nuclei (VPL, VPM, Po, Fig 7. (a)-(b)) of the thalamus 331  
 298 during anesthesia. The nRt neuron fired bursts containing 332  
 299 6-10 action potentials (Fig 7. (c)), while the recorded cortical 333  
 300 cells discharged mostly single spikes, spike doublets or triplets 334  
 301 (Fig. 7. (d)-(f)). During deep sleep and anesthesia brain 335  
 302 rhythms with lower frequencies (slow oscillation, 0.5-2 Hz; 336  
 303 delta, 2-4 Hz [25]), can be recorded from the thalamus and 337  
 304 cortex and the neuron discharges are time locked to the active 338  
 305 phases of these oscillations (Fig. x. (d)).

## 306 IV. CONCLUSION

307 *In vivo* electrophysiological measurements on rats with 340  
 308 silicon-based neural multielectrode arrays with extreme length, 341

robust mechanical parameters and adequate implantation and 309  
 targeting capabilities were performed in two separate labo- 310  
 ratories. Successful functional tests and histological studies 311  
 suggest that even though the probes presented here are thicker 312  
 and wider than commonly used silicon-based devices, they are 313  
 suitable for obtaining electronic interface with the cerebrum 314  
 of a small rodent. We suppose that since these probes are 315  
 of superior length, they are suitable candidates for acute *in* 316  
*vivo* experiences on animals with larger brain, such as cats or 317  
 primates, although further tests are necessary to ascertain this 318  
 assumption. 319

## V. ACKNOWLEDGEMENT

320 We are grateful to Mrs. Károlyné Payer, Mr. András 321  
 Straszner, Mr. Róbert Hodován and Mr. András Lőrincz for 322  
 their support in the clean room. We also wish to thank 323  
 Mr. Attila Nagy and Mr. István Réti for their help in chip 324  
 packaging. Useful and motivating discussions with Dr. László 325  
 Grand are greatly acknowledged. 326

## REFERENCES

- [1] J. S. Perlmutter and J. W. Mink, "Deep brain stimulation," *Annu. Rev. Neurosci.*, vol. 29, pp. 229-257, Aug. 2006. 328
- [2] D. M. Taylor, S. I. Tillery, and A. B. Schwartz, "Direct cortical control of 3D neuroprosthetic devices," *Science*, vol. 296, no. 5574, pp. 1829-1832, Apr. 2002. 329
- [3] F. H. Guenther, J. S. Brumberg, E. J. Wright, A. Nieto-Castanon, J. A. Tourville, M. Panko, R. Law, S. A. Siebert, J. L. Bartels, D. S. Andreasen, P. Ehirim, H. Mao, and P. R. Kennedy, "A wireless brain-machine interface for real-time speech synthesis," *PLoS ONE*, vol. 4, no. 12, p. e8218, Dec. 2009. 330
- [4] G. Kotzar, M. Freas, P. Abel, A. Fleischman, S. Roy, C. Zorman, J. M. Moran, and J. Melzak, "Evaluation of MEMS materials of construction for implantable medical devices," *Biomaterials*, vol. 23, no. 13, pp. 2737-2750, Jul. 2002. 331
- [5] A. Bragin, J. Hetke, C. L. Wilson, D. J. Anderson, J. Engel, Jr., and G. Buzsáki, "Multiple site silicon-based probes for chronic recordings in freely moving rats: Implantation, recording and histological verification," *J. Neurosci. Methods*, vol. 98, no. 1, pp. 77-82, May 2000. 332
- [6] P. J. Rousche and R. A. Normann, "Chronic recording capability of the Utah Intracortical Electrode Array in cat sensory cortex," *J. Neurosci. Methods*, vol. 82, no. 1, pp. 1-15, Jul. 1998. 333
- [7] K. Torab, T. S. Davis, D. J. Warren, P. A. House, R. A. Normann, and B. Greger, "Multiple factors may influence the performance of a visual prosthesis based on intracortical microstimulation: Nonhuman primate behavioural experimentation," *J. Neural Eng.*, vol. 8, no. 3, pp. 035001-1-035001-18, Jun. 2011. 334
- [8] M. Hajji-Hassan, V. P. Chodavarapu, and S. Musallam, "Microfabrication of ultra-long reinforced silicon neural electrodes," *IET Micro Nano Lett.*, vol. 4, no. 1, pp. 53-58, Mar. 2009. 335
- [9] D. T. Kewley, M. D. Hills, D. A. Borkholder, I. E. Opris, N. I. Maluf, C. W. Stormont, J. M. Bower, and G. T. A. Kovacs, "Plasma-etched neural probes," *Sens. Actuators A, Phys.*, vol. 58, no. 1, pp. 27-35, Jan. 1997. 336
- [10] P. J. Rousche, D. S. Pellinen, D. P. Pivin, Jr., J. C. Williams, R. J. Vetter, and D. R. Kirke, "Flexible polyimide-based intracortical electrode arrays with bioactive capability," *IEEE Trans. Biomed. Eng.*, vol. 48, no. 3, pp. 361-371, Mar. 2001. 337
- [11] A. Mercanzini, K. Cheung, D. L. Buhl, M. Boers, A. Maillard, P. Colin, J. C. Bensadoun, A. Bertsch, and P. Renaud, "Demonstration of cortical recording using novel flexible polymer neural probes," *Sens. Actuators A, Phys.*, vol. 143, no. 1, pp. 90-96, 2008. 338
- [12] V. S. Polikov, P. A. Tresco, and W. M. Reichert, "Response of brain tissue to chronically implanted neural electrodes," *J. Neurosci. Methods*, vol. 148, no. 1, pp. 1-18, Oct. 2005. 339
- [13] A. A. Fomani, M. Moradi, S. Assaf, and R. R. Mansour, "3D micro-probes for deep brain stimulation and recording," in *Proc. Annu. Int. Conf. IEEE Eng. Med. Biol. Soc.*, Sep. 2010, pp. 1808-1811. 340

- 375 [14] S. Felix, K. Shah, D. George, V. Tolosa, A. Tooker, H. Sheth, T. Delima,  
376 and S. Pannu, "Removable silicon insertion stiffeners for neural probes  
377 using polyethylene glycol as a biodegradable adhesive," in *Proc. Annu.*  
378 *Int. Conf. IEEE Eng. Med. Biol. Soc.*, Aug. 2012, pp. 871–874.
- 379 [15] D. Lewitus, K. L. Smith, W. Shain, and J. Kohn, "Ultrafast resorbing  
380 polymers for use as carriers for cortical neural probes," *Acta Biomater.*,  
381 vol. 7, no. 6, pp. 2483–2491, Jun. 2011.
- 382 [16] F. Gallyas, M. Hsu, and G. Buzsáki, "Four modified silver methods  
383 for thick sections of formaldehyde-fixed mammalian central nervous  
384 tissue: 'Dark' neurons, perikarya of all neurons, microglial cells and  
385 capillaries," *J. Neurosci. Methods*, vol. 50, no. 2, pp. 159–64, Nov. 1993.
- 386 [17] M. Welkenhuysen, A. Andrei, L. Ameye, W. Eberle, and B. Nuttin,  
387 "Effect of insertion speed on tissue response and insertion mechanics  
388 of a chronically implanted silicon-based neural probe," *IEEE Trans.*  
389 *Biomed. Eng.*, vol. 58, no. 11, pp. 3250–3259, Nov. 2011.
- 390 [18] K. Najafi and J. F. Hetke, "Strength characterization of silicon micro-  
391 probes in neurophysiological tissues," *IEEE Trans. Biomed. Eng.*,  
392 vol. 37, no. 5, pp. 474–481, May 1990.
- 393 [19] Z. Fekete, Z. Hajnal, G. Márton, P. Fürjes, and A. Pongrácz, "Fracture  
394 analysis of silicon microprobes designed for deep-brain stimulation,"  
395 *Microelectron. Eng.*, vol. 103, pp. 160–166, Mar. 2013.
- 396 [20] A. M. Dymond, L. E. Kaechele, J. M. Jurist, and P. H. Crandall, "Brain  
397 tissue reaction to some chronically implanted metals," *J. Neurosurg.*,  
398 vol. 33, no. 5, pp. 574–580, Nov. 1970.
- 399 [21] D. R. Merrill, M. Bikson, and J. G. Jefferys, "Electrical stimulation of  
400 excitable tissue: Design of efficacious and safe protocols," *J. Neurosci.*  
401 *Methods*, vol. 141, no. 2, pp. 171–198, Feb. 2005.
- 402 [22] G. Paxinos and C. Watson, *The Rat Brain in Stereotaxic Coordinates*,  
403 *Compact Sixth Edition*. San Diego, CA, USA: Academic, 2009.
- 404 [23] L. Hazan, M. Zugaro, and G. Buzsáki, "Klusters, neuroscope, NDman-  
405 ager: A free software suite for neurophysiological data processing and  
406 visualization," *J. Neurosci. Methods*, vol. 155, no. 2, pp. 207–216,  
407 Sep. 2006.
- 408 [24] M. A. Moffitt and C. C. McIntyre, "Model-based analysis of cortical  
409 recording with silicon microelectrodes," *Clinical Neurophysiol.*,  
410 vol. 116, no. 9, pp. 2240–2250, Sep. 2005.
- 411 [25] M. Steriade, "The corticothalamic system in sleep," *Frontiers Biosci.*,  
412 vol. 8, no. 1, pp. 878–899, 2003.

413 **Gergely Márton** received the M.Sc. degree in electrical engineering from  
414 the Budapest University of Technology and Economics, Műegyetem rakpart,  
415 Hungary, in 2010.

416 He is currently pursuing the Ph.D. degree with the János Szentágothai  
417 Doctoral School of Neuroscience, Semmelweis University, Budapest, Hun-  
418 gary, and is a Research Assistant with the Institute of Cognitive Neuroscience  
419 and Psychology, Research Centre for Natural Sciences, Hungarian Academy  
420 of Sciences, Budapest. His current research interests include development of  
421 neural interfaces with MEMS technologies.

422 **Zoltán Fekete** received the M.Sc. and Ph.D. degrees in electrical engineering  
423 from the Budapest University of Technology and Economics, Budapest,  
424 Hungary, in 2009 and 2013, respectively.

425 He is currently a Research Fellow with the Research Institute of Technical  
426 Physics and Material Science, Hungarian Academy of Sciences, Budapest. His  
427 current research interests include the development of MEMS devices, silicon  
428 and polymer microfluidics, and silicon-based neural microprobes.

**Richárd Fiáth** received the M.Sc. degree in electrical and computer engi-  
neering from the Faculty of Information Technology, Peter Pazmany Catholic  
University, Budapest, Hungary, in 2009.

He is currently pursuing the Ph.D. degree with the János Szentágothai  
Doctoral School of Neuroscience, Semmelweis University, Budapest, and  
is a Research Assistant with the Institute of Cognitive Neuroscience and  
Psychology, Research Centre for Natural Sciences, Hungarian Academy of  
Sciences, Budapest. His current research interests include silicon-based neural  
interfaces, investigation of thalamocortical interactions, and the physiology of  
sleep.

**Péter Baracska**y received the M.S. degree in neurobiology from Eötvös  
Lóránd University, Budapest, Hungary, in 2007.

He was a Research Assistant with the Department of Medical Chemistry,  
University of Szeged, Szeged, Hungary, from 2010 to 2011. He is currently  
with the Bay Zoltan Nonprofit Ltd. for Applied Research, Budapest, and is  
currently a Graduate Student with the Institute of Biology, Eötvös Lóránd  
University, Egyetem tér, Hungary.

**István Ulbert** received the M.Sc. degree in technological physics from the  
Technical University of Budapest, Budapest, Hungary, in 1988, the M.D.  
degree from the Medical School, Semmelweis University, Budapest, in 1997,  
and the Ph.D. degree in neurosciences from the Doctoral School, Semmelweis  
University, in 2002.

He gained scientific experience as a Research Associate with the Albert  
Einstein College of Medicine, Department of Neuroscience, Bronx, NY, USA,  
from 1994 to 1996, as a Post-Doctoral Fellow with Stanford University  
Medical School, Department of Neurosurgery, Stanford, CA, USA, from 1997  
to 2000, and as an Instructor of radiology with Harvard University Medical  
School, Department of Radiology, Massachusetts General Hospital, Boston,  
MA, USA, from 2000 to 2003. He is currently a Senior Research Scientist and  
a Group Leader with the Institute of Cognitive Neuroscience and Psychology,  
Research Centre for Natural Sciences, Hungarian Academy of Sciences,  
Budapest, and an Associate Professor with the Faculty of Information Technol-  
ogy, Pázmány Péter Catholic University, Budapest. He has co-authored over  
50 articles in peer-reviewed journals and over 250 publications in the forms  
of conference proceedings, book chapters, posters, and lectures. His current  
research interests include the development of implantable cortical biosensors  
for human and animal applications and the investigation of intracortical  
generators of brain oscillations.

**Gábor Juhász**, photograph and biography are not available at the time of  
publication.

**Gábor Battistig**, photograph and biography are not available at the time of  
publication.

**Anita Pongrácz** received the M.Sc. degree in engineering physics from the  
Technical University of Budapest, Budapest, Hungary, in 2004.

She was a Baseline Process Engineer with the University of California,  
Berkeley Microfabrication Laboratory, Berkeley, CA, USA, from 2006 to  
2007. Her main responsibilities were to design, fabricate, test, and evaluate  
CMOS test devices. She received the Ph.D. degree in 2010 and is currently a  
Research Fellow with the Institute of Technical Physics and Material Science,  
Hungarian Academy of Sciences, Budapest. Her current research interests  
include microfabrication of neuroMEMS devices.

429

430

431

432

433

434

435

436

437

438

439

440

441

442

443

444

445

446

447

448

449

450

451

452

453

454

455

456

457

458

459

460

461

462

463

464

465

466

467

468

469

470

471

472

473

474

475

476

477

478

479

480

481

482

483

484

485

486

487

488

489

490

491

492

493

494

495

496

497

498

499

500

501

502

503

504

505

506

507

508

509

510

511

512

AQ:3

## AUTHOR QUERIES

- AQ:1 = Images 1, 3, and 4 are not cited in the text. Please indicate where they should be cited.
- AQ:2 = Please confirm whether “kirke” is “Kirke” or “Kipke.”
- AQ:3 = Please provide biography for the authors “Gábor Juhász and Gábor Battistig” if desired.

IEEE  
Proof